Biogeosciences Discuss., doi:10.5194/bg-2016-521, 2017
Manuscript under review for journal Biogeosciences
Published: 16 January 2017

Biogeosciences Discussions Open Access EGU

Quantifying nutrient uptake as driver of rock weathering in forest ecosystems by magnesium stable isotopes

David Uhlig[1], Jan A. Schuessler[1], Julien Bouchez[1,2], Jean L. Dixon[1,3], Friedhelm von Blanckenburg[1,4]

[1]GFZ German Research Centre for Geosciences, Earth Surface Geochemistry, Telegrafenberg, 14473 Potsdam, Germany
[2]Present address: IPGP Institut de Physique du Globe de Paris, rue Jussieu, 75238 Paris cedex 05, France
[3]Present address: Montana State University, Department of Earth Sciences, Bozeman, Montana 59717, USA
[4]Freie Universität Berlin, Institute of Geological Sciences, Malteserstr. 74-100, 12249 Berlin, Germany

Correspondence to: David Uhlig (david.uhlig@gfz-potsdam.de)

Abstract Plants and soil microbiota play an active role in rock weathering and potentially couple weathering at depth with erosion at the soil surface. The nature of this coupling is still unresolved because we lacked means to quantify the passage of chemical elements from rock through higher plants. In a temperate forested landscape of the Southern Sierra Critical Zone Observatory (SSCZO), California, we measured magnesium (Mg) stable isotopes that are sensitive indicators of Mg utilisation by biota. We find that Mg is highly bio-utilised: 50-100 % of the Mg released by chemical weathering is taken up by forest trees. To estimate the tree uptake of other bio-utilised elements (K, Ca, P and Si) we compared the dissolved fluxes of these elements and Mg in rivers with their solubilisation fluxes from rock (rock dissolution flux minus secondary mineral formation flux). We find a deficit in the dissolved fluxes throughout, that we attribute to the nutrient uptake by forest trees. Therefore both the Mg isotopes and the flux comparison suggests that a substantial part of the major element weathering flux is consumed by the tree biomass. This isotopic and elemental compartment separation is preserved only if the mineral nutrients contained in biomass are prevented from re-dissolution after litter fall, showing that these nutrients have been removed as "solid" biomass. The enrichment of ^{26}Mg over ^{24}Mg in tree trunks relative to leaf litter suggests that this removal occurs mainly in coarse woody debris (CWD). Today, CWD is exported from the ecosystem by tree logging. Over pre-anthropogenic weathering time scales, a similar removal flux might have been in operation in the form of natural erosion of CWD. Regardless of the removal mechanism, our data provides the first direct quantification of biogenic uptake following weathering. We find that Mg and other bio-elements are taken up by trees at up to 7 m depth, and surface recycling of all bio-elements but P is minimal. Thus, in the watersheds of the SSCZO in which weathering is fast and kinetically-limited, the coupling between erosion and weathering might be established by bio-elements that are taken up by trees, not recycled and missing in the dissolved river flux due to erosion as CWD and as leaf-derived bio-opal for Si. We suggest that the partitioning of a biogenic weathering flux into eroded plant debris might represent a significant global contribution to element export after weathering in eroding mountain catchments that are characterised by a continuous supply of fresh mineral nutrients.

Biogeosciences Discuss., doi:10.5194/bg-2016-521, 2017
Manuscript under review for journal Biogeosciences
Published: 16 January 2017

1 Introduction

In continuously eroding landscapes, the mass loss of particles by erosion and solutes by drainage needs to be balanced over a kilo year time scale by the conversion of rock into regolith, where we define regolith as the entire weathering zone above bedrock, including topsoil (Dixon and von Blanckenburg, 2012). The advance of the weathering front at depth is thus coupled to surface denudation (Brantley and Lebeveda, 2011). It has been hypothesised that biotic processes contribute towards this coupling (Brantley et al., 2011). If the nutrient demand of plants and soil microbes is linked to the advance of the weathering front, investigating the dependence of nutrient fluxes on the weathering regime allows for a test of the biogenic weathering hypothesis.

The way weathering systems operate can be characterised by two endmembers, each associated with a specific pattern of nutrient dynamics. In the supply-limited regime, the transfer of nutrient-bearing mineral grains from rock into the regolith is so slow that their complete dissolution decreases the mineral nutrient status of the regolith and plants and soil microbes are nourished by re-mineralisation and recycling of nutrients from plant litter (Lang et al., 2016; Vitousek and Farington, 1997) and by atmospheric inputs (Vitousek and Farington, 1997). In the kinetically-limited regime, ongoing erosion rejuvenates regolith (Porder et al., 2007), such that the rate of supply outpaces the weathering of minerals (West et al., 2005). The supply of solutes by chemical weathering into soil solutions ensures that nutrients are readily available for plant uptake from regolith water. In this regime of long-lasting erosion, a fraction of these nutrients is lost after bio-utilisation in plant debris such as leaf litter and coarse woody debris (CWD). The plant litter can also be re-mineralised, so that nutrients are lost by drainage in the dissolved form. If erosion of plant debris outpaces nutrient leaching, nutrients are eroded in leaf litter by erosion or stochastically as woody matter in landslides. To replace either loss, nutrients are uplifted from subsoil layers (Jobbagy and Jackson, 2001). To facilitate the uplift from subsoil in the kinetically-limited regime, plants and soil microbes can stimulate chemical weathering rates by decreasing the rhizospheric pH through respiration of CO_2 and the excretion of weathering agents (Brantley et al., 2011). Moreover, the symbiosis of roots with mycorrhiza fungi (Landeweert et al., 2001) enables plants to directly assimilate nutrients from primary minerals (Jongmans et al., 1997). Here we explore this hypothesis in a kinetically-limited mountain setting using isotopic and geochemical techniques.

The stable isotopes of magnesium (Mg) - a macronutrient for plants and a major constituent of the bulk silicate Earth - are suitable to trace these cycles. Unless fractionated by the neoformation of secondary minerals (Wimpenny et al., 2014), the $^{26}Mg/^{24}Mg$ ratio is mainly shifted towards high values during nutrient uptake by plants (Black et al., 2008; Bolou-Bi et al., 2012; Mavromatis et al., 2014), and the residual dissolved Mg is shifted towards the complementary low ratio. These two compartments remain separated if a fraction of the Mg is eroded as mainly CWD after utilisation and is not released back into solution. In that case the isotope ratio serves as a proxy for the catchment wide net nutrient uptake flux, where “net” excludes re-mineralisation and recycling. Here we use an isotope mass balance model (Bouchez et al., 2013) to quantify what the relative

Biogeosciences Discuss., doi:10.5194/bg-2016-521, 2017
Manuscript under review for journal Biogeosciences
Published: 16 January 2017

fluxes are that export Mg after rock weathering: uptake into plants, export as solute, or erosion in particles including minerals and a substantial CWD fraction at three forested headwater catchments.

2 Methods

2.1 Study site

Our study sites comprise three catchments at Providence Creek, Sierra Nevada, USA and are part of two monitoring programs: Kings River Experimental Watersheds and Southern Sierra Critical Zone Observatory (SSCZO). The extensive SSCZO dataset is highly suited for nutrient cycling studies in forest ecosystems and provides evidence that rock phosphorus might be growth-limiting (Hahm et al., 2014). Our study sites are underlain by granodiorite bedrock (Bateman and Wones, 1972) and mantled by weakly developed soils comprising Entisols and Inceptisols (Bales et al., 2011). Soil water and stream water pH ranges from 5.5 to 7. We estimate the soil production rate from the total denudation rate from cosmogenic nuclides which is ~220 t km^{-2} yr^{-1} (Dixon et al., 2009). This weathering regime is kinetically-limited and soils are only partially depleted in mineral nutrients. In contrast, the dust input is minor at 1 to 10 t km^{-2} yr^{-1} (Mahowald et al., 2005) and can be neglected in this study. The main vegetation cover is Sierran mixed conifer comprising *Pinus ponderosa*, *Pinus lambertiana*, *Abies concolor* and *Libocedrus decurrens* (McCorkle et al., 2016).

2.2 Analytical methods

The chemical composition of soil, saprolite and rock samples were analysed by X-ray fluorescence spectrometry (XRF, Panalytical Axios Advanced) on fused tablets at GFZ Potsdam or by Acme Labs, Canada, with uncertainties better than 10 % relative. Additional concentration data was compiled from Hahm et al. (2014) and Riebe and Granger (2013). Element concentrations in plant material were analysed by an Inductively Coupled Plasma Optical Emission Spectrometer (ICP-OES, Varian 720ES) with uncertainties better than 15 %, after complete dissolution in HNO_3/H_2O_2 in PFA vials on a hotplate or using a microwave digestion system as successfully applied in previous Mg isotope studies (e.g., Bolou-Bi et al., 2012). Dissolved element concentrations in water samples were analysed by ICP-OES following the procedure described in Schuessler et al. (2016), Inductively Coupled Plasma Quadrupole Mass Spectrometry (Q-ICP-MS, Thermo iCAP-Q), and ion chromatography (Thermo Dionex DX-120) with uncertainties better than 10 %, respectively. All data of samples and reference materials (for assessment of analytical uncertainties) are reported in Tables S1 to S3.

2.3 Mg isotope analyses by MC-ICP-MS

Mg stable isotope analyses have been performed at GFZ Potsdam, Helmholtz Laboratory for the Geochemistry of the Earth Surface (HELGES). Samples and reference materials were digested in PFA vials using ultra-pure acid mixtures (HF, HCl, HNO_3, H_2O_2). The exchangeable Mg fraction of soil and saprolite samples was obtained by a 1 M NH_4OAc extraction (Arunachalam et al., 1996). This procedure was specifically tested for Mg isotope measurements (Bolou-Bi et al., 2012). After

Biogeosciences Discuss., doi:10.5194/bg-2016-521, 2017
Manuscript under review for journal Biogeosciences
Published: 16 January 2017

extraction, the residual solids were analysed after HF/HNO_3 total digestion. Before isotope analysis, Mg was separated from other matrix elements by column chromatography (AG50W-X12 resin) following the procedure described in Pogge von Strandmann et al. (2011). Matrix elements were eluted with 1 M HNO_3, and then Mg was collected by elution with 2 M HNO_3. Purity of the Mg solutions as well as Mg yields were verified by analyses of final Mg-containing solutions using ICP-OES or Q-ICP-MS. Mg isotope ratios were measured with a Multi Collector Inductively Coupled Plasma Mass Spectrometer (MC-ICP-MS, Thermo Neptune). All sample solutions were diluted in 0.3 M HNO_3, where the samples Mg concentration was closely matched to those of the bracketing standard DSM-3. Results are expressed as the ‰ difference of the Mg isotope ratio of the sample relative to the DSM-3 isotope reference material (Galy et al. 2003) using the delta notation: $\delta^{26}Mg = [(^{26}Mg/^{24}Mg)_{sample}/(^{26}Mg/^{24}Mg)_{DSM3} - 1] \times 1000$. The uncertainty is estimated to be ±0.10 ‰ (2SD) for $\delta^{26}Mg$, respectively, based on repeat measurements on reference materials (Tables S1 to S3).

2.4 Mg isotope analyses by fsLA-MC-ICP-MS

The micro-scale Mg isotope composition of individual minerals (amphibole and biotite) was determined on a thin section of sample BP-0c (from the bedrock-saprolite interface) by UV femtosecond laser ablation coupled to a Thermo Neptune MC-ICP-MS (fs LA-MC-ICP-MS, *Fem2*) at GFZ Potsdam. Instrumentation, data acquisition and evaluation procedures are described in detail in Schuessler and von Blanckenburg (2014). Laser ablation was performed on individual mineral grains with a spatial resolution of less than 200 x 200 µm surface area with less than 10 µm crater depth. The laser beam with a diameter of about 25 µm was scanned across the mineral surface to adapt to the irregular shape of the grains and cracks with repetition rates between 13 to 20 Hz. The high mass resolution mode of the MC-ICP-MS was used for Mg isotope ratio measurements. With high mass resolution, isobaric interferences ($^{52}Cr^{2+}$ on $^{26}Mg^{+}$, $^{50}Ti^{2+}$ and $^{50}Cr^{2+}$ on $^{25}Mg^{+}$, or $^{48}Ca^{2+}$ and $^{48}Ti^{2+}$ on $^{24}Mg^{+}$) can be resolved from Mg isotopes (Meng-Ning et al., 2016; Oeser et al., 2014). Mass bias correction was performed using the komatiite glass GOR132-G as bracketing standard. Using a $\delta^{26}Mg$ value for GOR132-G of -0.17 ‰ relative to DSM-3 (Oeser et al., 2014), we converted results to δ-values relative to DSM-3. Based on our current experience, we conservatively estimate the uncertainty of the fsLA-MC-ICP-MS method for Mg isotope ratios to be better than ±0.25 ‰ (2SD) for $\delta^{26}Mg$. Repeat measurements on reference material BHVO-2G (basaltic glass) (average $\delta^{26}Mg = -0.07 \pm 0.18$ ‰, 2SD, n=18) agree within uncertainties to published values (Fig. 1) for this reference material (−0.20 ± 0.07 ‰, Meng-Ning et al., 2016). Results of biotite and amphibole analyses are presented in Fig. 1. Photomicrographs (Fig. 2) show representative analysis locations in amphibole and biotite before and after laser ablation.

3 Results

3.1 Mg isotopic composition of ecosystem compartments

The Mg isotopic composition (Fig. 3, Tables S1 to S3) of mean bulk rock ($\delta^{26}Mg_{rock}$ = -0.22 ‰ ± 0.10 ‰, 2SD) is identical within uncertainties to mean bulk regolith ($\delta^{26}Mg_{reg}$ = -0.15 ‰ ± 0.13 ‰, 2SD) and mean suspended sediment

Biogeosciences Discuss., doi:10.5194/bg-2016-521, 2017
Manuscript under review for journal Biogeosciences
Published: 16 January 2017

($\delta^{26}Mg_{susp.sed}$ = -0.30 ‰ ± 0.16 ‰, 2SD). Results of analyses on biotite and amphibole on a thin section of rock sample BP-0c indicate that Mg-bearing minerals in the bedrock are not distinguishable in $\delta^{26}Mg$ within analytical uncertainties and are also identical to the bulk bedrock value of sample BP-0c (Fig. 1). $\delta^{26}Mg$ in wood from growing trees ranges from -0.21 to +0.16 ‰, and $\delta^{26}Mg$ in growing foliage is lower than wood, i.e., -0.72 to -0.10 ‰. $\delta^{26}Mg$ of foliage, twigs, bark, and needles sampled from the forest floor and from the gauged creek sediment pond are within the range found in living foliage. The intra-plant differences are consistent with previous studies that have shown that during translocation ^{24}Mg is preferred by the foliage whereas ^{26}Mg is preferred by wood (Black et al., 2008; Bolou-Bi et al., 2012). Despite the low $\delta^{26}Mg$ in foliage, bulk tree ($\delta^{26}Mg_{tree} \approx$ -0.07 ‰, see mass balance calculation in Appendix A) is not distinguishable from bulk soil and rock. Only Mg in creek water ($\delta^{26}Mg_{diss}$ = -0.76 ‰ ± 0.11 ‰, 2SD) and exchangeable Mg from soil and saprolite ($\delta^{26}Mg_{exch}$ = -0.68 ‰ ± 0.36‰, 2SD) differ from the solid compartments. $\delta^{26}Mg_{diss}$ is remarkably constant throughout one hydrological water year and is in the range of global rivers draining silicate catchments (Tipper et al., 2012 and references therein). Results of element concentration measurements in rock, saprolite, soil, vegetation, water, and sediment samples are reported together with field measurement data (pH, temperature, conductivity, discharge, alkalinity) in tables S1 to S3.

4 Discussion

4.1 Mg isotope fractionation by clay formation

Neoformation of Mg-clays is a mechanism that preferentially removes ^{26}Mg from soil solution and enriches this heavy isotope in Mg-clays such as smectite, illite or vermiculite (Wimpenny et al., 2014; Ryu et al., 2016). Clay formation is thus a potential cause for the low $\delta^{26}Mg_{diss}$ observed in the Providence Creek streams. However, Mg-clay abundances are beneath the 5 % detection limit of XRD analysis and their absence was confirmed by thermodynamic modelling (PhreeqC). We use an isotope mass balance based on bulk soil Mg isotope composition to evaluate whether the low $\delta^{26}Mg$ of dissolved Mg could, however, be due to preferential incorporation of ^{26}Mg into small amounts of Mg-clay. The abundance of Mg-clay was beneath the limit of detection of XRD. In an isotope mass balance (Eq. (1)) we assign $\delta^{26}Mg_{bulk\ soil}$ the value of the isotopically heaviest soil sample (-0.05 ‰, see Table S3), which has the potential to be most affected by Mg-clay formation; and for primary minerals $\delta^{26}Mg_{prim}$ we use the rock mean $\delta^{26}Mg_{rock}$ (-0.22 ‰, Table S3).

$$\delta^{26}Mg_{bulk\ soil} = \delta^{26}Mg_{sec} \cdot f_{sec}^{Mg} + \delta^{26}Mg_{prim} \cdot \left(1 - f_{sec}^{Mg}\right) \quad (1)$$

We first solve Eq. (1) for $\delta^{26}Mg_{sec}$ with f_{sec}^{Mg} of 4 % which corresponds to the fraction of Mg derived from 5 % Mg-clay (XRD detection limit) and 20 % amphibole/biotite in bulk soil (Appendix B). Soil Mg isotopes can only be explained if $\delta^{26}Mg$ in secondary minerals ($\delta^{26}Mg_{sec}$) ≥ 4 ‰, which is unlikely (Wimpenny et al., 2014). Second, we solve Eq. (1) for f_{sec}^{Mg} by using the maximum published $\delta^{26}Mg_{sec}$ of 0.5 ‰ (Ryu et al., 2016 and references therein). This clay value is also consistent with a

Biogeosciences Discuss., doi:10.5194/bg-2016-521, 2017
Manuscript under review for journal Biogeosciences
Published: 16 January 2017

Rayleigh-type mass balance constrained by the $\delta^{26}Mg$ of measured stream water and bulk rock as source Mg using $\alpha_{solid\text{-}solution}$ = 1.00054 (Ryu et al., 2016). In this case the bulk soil Mg-clay content were 30 %, far in excess of our XRD analyses (Appendix B).

Therefore, the low $\delta^{26}Mg$ of dissolved Mg cannot be attributed to incorporation into clays. The remaining process that depletes soil water in ^{26}Mg is preferential uptake of ^{26}Mg by plants (Black et al., 2008; Bolou-Bi et al., 2012) associated with an isotope fractionation factor between plant Mg and dissolved Mg in the soil solution, expressed as $\Delta^{26}Mg_{plant\text{-}diss}$.

4.2 Mg tree uptake fractions from an isotope mass balance

We quantify the fraction of Mg uptake by higher plants (f_{uptake}^{Mg}) by a closed-system mass balance by Eq. (2) (Black et al., 2008; Johnson et al., 2004):

$$f_{uptake}^{Mg} = \frac{\delta^{26}Mg_{rock} - \delta^{26}Mg_{diss}}{\Delta^{26}Mg_{plant-diss}}. \quad (2)$$

In Eq. (2) we use the isotopic difference between the "initial" $\delta^{26}Mg_{diss}$, and $\delta^{26}Mg_{diss}$ that has been modified from the initial soil solution by Mg uptake into plants. Since we do not know the initial $\delta^{26}Mg_{diss}$ we use $\delta^{26}Mg_{rock}$ as a proxy for this weathering solution, assuming congruent dissolution (Bouchez et al., 2013). It can be excluded that differences in primary mineral $\delta^{26}Mg$ lead to preferential release of specific $\delta^{26}Mg$, based on fs-laser ablation data of biotite and amphibole, the main Mg carriers, which are similar to $\delta^{26}Mg$ of bulk bedrock (Sect. 2.4 and Fig. 1). The f_{uptake}^{Mg} calculated here presents a minimum estimate ("net") of the total uptake fraction, as it does not include a fraction of Mg that is potentially recycled back into solution after uptake through Mg release from plant litter. We note that f_{uptake}^{Mg} calculated by Eq. (2) is mathematically equivalent to the results of the steady state flow-through reactor model of Bouchez et al. (2013) (see below), but here f_{uptake}^{Mg} reflects an instantaneous mass balance and does not depend on a steady state of fluxes, but applies only to an idealised closed system where plants exchange Mg with regolith water.

We can also describe both uptake and removal of Mg by a flow-through reactor isotope model (Bouchez et al., 2013). Combining Eq. 3c, Eq. 3d and Eq. 5e from Bouchez et al. (2013) and assuming that no Mg is incorporated into secondary minerals leads to Eq. (3):

$$\frac{\delta^{26}Mg_{rock} - \delta^{26}Mg_{diss}}{\Delta^{26}Mg_{plant-diss}} = \frac{U^{Mg} - S_{org}^{Mg}}{S_{rock}^{Mg} + S_{prim}^{Mg}} = \frac{E_{org}^{Mg}}{S_{rock}^{Mg} + S_{prim}^{Mg}}. \quad (3)$$

The denominator in Eq. (3) represents the sum of the Mg supply fluxes from rock dissolution (S_{rock}^{Mg}) at the weathering front and from primary minerals remaining in the regolith (S_{prim}^{Mg}). The flux term U^{Mg} quantifies the Mg uptake flux by trees. S_{org}^{Mg}

Biogeosciences Discuss., doi:10.5194/bg-2016-521, 2017
Manuscript under review for journal Biogeosciences
Published: 16 January 2017

represents the flux of Mg from re-mineralisation of plant litter that is either recycled back into the plants, or discharged into the river. Note that the left-hand and middle term of Eq. (3) is identical to the determination of the relative Mg uptake flux f_{uptake}^{Mg} by a closed system mass balance (Eq. (2)). The isotope ratios are thus set by the Mg uptake flux by trees relative to the solubilisation flux of Mg by chemical weathering. The combination of the middle term in Eq. (3) with its isotopic expression in the left-hand term does not require fluxes that are steady with time and is applicable to the transient growth of biomass. The equation can be expanded into the right-hand steady state term by assuming that in a steadily eroding weathering regime over the time scale of soil formation Mg initially released by weathering is also removed from the ecosystem by a) the dissolved export, and b) particulate export in plant litter including CWD (E_{org}^{Mg}). As the formation of Mg-clays or the dissolution of carbonates do not affect Mg fluxes at our study sites (Sect. 3.2, Bateman and Wones, 1972), an isotope difference between rock and dissolved Mg only emerges if a substantial fraction of isotopically fractionated Mg is exported in plant litter or CWD.

To estimate a range for f_{uptake}^{Mg} (Eq. (2)), or, at steady state, E^{Mg} (Eq. (3)), we applied Eq. (2) and Eq. (3) to all individual Providence Creek water samples by using a minimum and maximum $\Delta^{26}Mg_{plant\text{-}diss}$ of 0.50 ‰ (Opfergelt et al., 2014) and 0.68 ‰ (Black et al., 2008), respectively, and considered the analytical uncertainty on $\delta^{26}Mg$ of 0.10 ‰ (2SD). The difference of 0.5 ‰ we found between $\delta^{26}Mg_{diss}$ and $\delta^{26}Mg_{rock}$ shows that 50 % to 100 % of the Mg initially released by chemical weathering is taken up by trees, and is eventually eroded in plant litter and CWD. Consequently, because of the high fraction of Mg uptake, the mean weighted $\delta^{26}Mg_{tree}$ is identical to bulk rock (Fig. 3). Therefore, at Providence Creek Mg is strongly bio-utilised.

Even though bulk tree $\delta^{26}Mg$ is higher than $\delta^{26}Mg_{diss}$, its composition is close to that of the parent rock and soil (Fig. 3). The reason is that during tree growth, the Mg taken up is partitioned into a high $\delta^{26}Mg$ compartment in woody plant matter, and a low compartment in leaves and needles. However, to explain the deficit in ^{26}Mg in dissolved stream Mg, a high $\delta^{26}Mg$ compartment has to be eroded, which could be located in the plant debris contained in forest floor material and river particulate matter. We analysed $\delta^{26}Mg$ of foliage, twigs and bark sampled from the forest floor and a sediment pond containing the erosion products of the ecosystem. Forest floor and sediment pond needles (Table S2) are isotopically light as expected, given that needles become isotopically lighter as they age (Bolou-Bi et al., 2012). Twigs (Table S2) are isotopically light too. This finding is in contrast with the isotope composition we found in living wood (Fig. 3), and isotopically heavy Mg published for wood (Black et al., 2008; Bolou-Bi et al., 2012). The low $\delta^{26}Mg$ of the fine twigs (diameter ~3 mm) is explained by their Mg isotopic composition being dominated by bark for which we also found low $\delta^{26}Mg$, consistent with Chapela Lara et al. (2016). Regardless, the compartment containing the required high $\delta^{26}Mg$ fraction is not contained in these samples.

However, the high $\delta^{26}Mg$ fraction is found in the wood of tree trunks (Fig. 3, Table S2). We interpret this observation to mean that the high $\delta^{26}Mg$ fraction contained in solid plant debris is exported only to a minor fraction contained in eroded foliage,

Biogeosciences Discuss., doi:10.5194/bg-2016-521, 2017
Manuscript under review for journal Biogeosciences
Published: 16 January 2017

and to a large fraction contained in exported tree trunks. Our isotope mass balance allows for two export mechanisms: transient growth of tree biomass following logging and mechanical removal of tree trunks (middle term in Eq. (3)); or natural erosion of coarse woody debris (CWD), at steady state with its uptake, with only minor leaching of Mg (right-hand term in Eq. (3)). We return to discussing these mechanisms in Sect. 3.9.

4.3 Mg weathering fluxes from an isotope mass balance

The fact that Mg is highly bio-utilised and eventually eroded as CWD dictates that the dissolved Mg export fraction is low. We use the isotope mass balance model (Bouchez et al., 2013) to calculate the dissolved Mg export fraction (w_{iso}^{Mg}) by Eq. (4) and report the data in Table S4b:

$$w_{iso}^{Mg} = \frac{\delta_{topsoil}^{Mg} - \delta_{rock}^{Mg}}{\delta_{topsoil}^{Mg} - \delta_{diss}^{Mg}}. \quad (4)$$

This fraction reflects the Mg solute export from the whole system relative to the total Mg export of solutes and particulates in primary and secondary minerals plus plant litter. Estimating w_{iso}^{Mg} does not depend on knowing isotope fractionation factors.

We use the mean δ^{26}Mg of unweathered rock, spatial- and time-integrated creek water of the individual Providence Creek sites (P301, P303, P304), and mean bulk topsoil from the P301 soil profile and the soil-saprolite Balsam Profile (Fig. 3). Topsoil was chosen to be more representative of exported particulate matter compared to creek sediment, because hydrodynamic sorting in the creek channel does not allow representative sampling of sediment. Because δ^{26}Mg of topsoil and bulk rock are identical within their analytical uncertainties we calculate a potential upper boundary of the possible Mg relative weathering flux w_{iso}^{Mg} by propagating the analytical uncertainties as in Bouchez et al. (2013). We determined w_{iso}^{Mg} only for Mg and did not attempt isotope analyses of other bio-elements. The analysis of stable potassium (K) isotopes is not yet routine due to analytical limitations (Wang and Jackobsen, 2016). Isotopic fractionation of calcium (Ca) during uptake by plants does not appear to sufficiently shift the isotopic composition of water from that of its source rock as indicated by global compilations (Bouchez et al., 2013; Fantle and Tipper, 2014). Phosphorus (P) has only one stable isotope, and silicon (Si) isotopes fractionate by neoformation of secondary minerals or adsorption onto e.g. goethite (both are present in minor amounts at Providence Creek as determined by thermodynamic modelling (PhreeqC)) into the same direction as Si uptake by plants (Opfergelt and Delmelle, 2012).

Our results show that according to Eq. (4) only 14 ± 13 % of Mg is exported from the weathering zone in the dissolved form (Fig. 4). Therefore, the complementary 86 % of Mg is exported predominantly in silicate minerals and in a substantial proportion of CWD.

Biogeosciences Discuss., doi:10.5194/bg-2016-521, 2017
Manuscript under review for journal Biogeosciences
Published: 16 January 2017

4.4 Elemental dissolved river fluxes

Next, we calculate an independent estimate of the relative dissolved Mg river flux (w^{Mg}_{diss}) that allows comparison with the isotope-based dissolved Mg export (w^{Mg}_{iso}). We also calculate the dissolved river flux w^{X}_{diss} for the elements (X) Si, K, Ca, and P. The non-normalised dissolved annual river fluxes for these elements (W^{X}_{diss}) are derived from Eq. (5), which is the sum of the catchment area (A) normalised products of daily dissolved creek water concentrations ($[X]_{diss_i}$) and daily discharge (Q_i) of one hydrological water year:

$$W^{X}_{diss} = \sum_{i=1}^{365} \frac{[X]_{diss_i} \cdot Q_i}{A}. \quad (5)$$

Since we lack daily resolution $[X]_{diss}$ data and our sampling years (2004-2010) differ from the hydrological water years (2010-2014) for which daily discharge is available (http://criticalzone.org/sierra/data), we use linear regression to determine daily $[X]_{diss_i}$. We calculate mean discharge values from 15 days before to 15 days after each of our seven $[X]_{diss}$ data points for all hydrological water years 2004 to 2010 and calculate annual W^{X}_{diss} for the individual hydrological water years 2004-2010 by applying Eq. (5). We calculate an average of all hydrological water years 2004 to 2010 to derive W^{X}_{diss} (Table S4a). For example, catchment average W^{Mg}_{diss} range from about 7700 to 28,000 t km^{-2} yr^{-1}.

To allow comparison between flux estimates of different elements, we normalise the measured fluxes to the same metric. We use the elemental regolith production rate (RP^X, Table S4a), which quantifies the transfer of an element X from bedrock to regolith at the weathering front (Bouchez et al., 2013) by Eq. (6):

$$RP^X = D \cdot [X]_{rock}. \quad (6)$$

Here, we use the total denudation rate (D) from cosmogenic *in situ* ^{10}Be concentration from Dixon et al. (2009). Using D of 220 t km^{-2} yr^{-1} for all catchments and $[Mg]_{rock}$ of 1.9 weight-%, RP^{Mg} is about 175,000 mol km^{-2} yr^{-1}. The normalised dissolved river fluxes (w^{X}_{diss}) are calculated by Eq. (7) (Bouchez et al., 2013) and reported in Table S4b:

$$w^{X}_{diss} = \frac{W^{X}_{diss}}{RP^X}. \quad (7)$$

w^{Mg}_{diss} amounts to 4-16 % (Fig. 4) and is similarly low as w^{Mg}_{iso} of ca. 14 %, supporting the notion that a substantial fraction of dissolved Mg is taken up by plants and subsequently eroded as CWD.

Biogeosciences Discuss., doi:10.5194/bg-2016-521, 2017
Manuscript under review for journal Biogeosciences
Published: 16 January 2017

4.5 Net elemental solubilisation fluxes in the weathering zone

To test the interpretation that a substantial fraction of Mg and other bio-elements (X) are exported as plant litter and CWD we compare the relative dissolved export fluxes of Mg w_{diss}^{Mg} and w_{iso}^{Mg} to the normalised net solubilisation flux (w_{τ}^{Mg}, Table S4b). The non-normalised net solubilisation flux (W_{τ}^{X}) is determined by Eq. (8) and reported in Table S4a:

$$W_{\tau}^{X} = D \cdot (-\tau_{Zr}^{X}) \cdot [X]_{rock}. \quad (8)$$

W_{τ}^{X} is defined as the flux of release of X from minerals undergoing weathering, minus the flux of incorporation of X into new minerals formed during weathering reactions (e.g. clays). W_{τ}^{X} is derived from total denudation rate (D), loss fractions (τ^{X}), and bedrock concentrations ($[X]_{rock}$). The loss fraction (τ^{X}) quantifies the depletion ($\tau < 0$) or enrichment ($\tau > 0$) of an element X relative to unweathered bedrock (Riebe et al., 2003). τ^{X} is determined by Eq. (9):

$$\tau_{Zr}^{X} = \frac{[Zr]_{unweathered\ bedrock}}{[Zr]_{weathered\ regolith}} \cdot \frac{[X]_{weathered\ regolith}}{[X]_{unweathered\ bedrock}} - 1. \quad (9)$$

Zr is used as the immobile element. In addition to the data set of this study, additional data (Hahm et al., 2014; Riebe and Granger, 2013) have been used to obtain the most representative bedrock concentrations and are reported with our data in Table S3.

The net solubilisation flux W_{τ}^{X} is determined by Eq. (8) for each of the Providence Creek catchments and ranges from 41,000 to 75,000 t km^{-2} yr^{-1} for Mg. Since τ^{X} is relatively uniform across the sampled soil-saprolite profile (Fig. 6) mean τ^{X}-values based on soil and saprolite data from Hahm et al. (2014) and Riebe and Granger (2013) (Table S3) have been used. Only τ^{P} is strongly depth-dependent (Fig. 6). Hence the values used in this study are from the mineral topsoil at 13-26 cm depth. The normalised net solubilisation flux (w_{τ}^{X}) is determined by Eq. (10):

$$w_{\tau}^{X} = \frac{W_{\tau}^{X}}{RP^{X}}. \quad (10)$$

w_{τ}^{X} is equal to $-\tau_{Zr}^{X}$ and the regolith production rate of element X (RP^{X}) at depth is equal to the total denudation rate of element X.

w_{τ}^{Mg} is much higher than w_{iso}^{Mg} and w_{diss}^{Mg} and amounts to ~40 % (Fig. 4), meaning that in the regolith 40 % of the Mg supplied from rock is transferred into the dissolved form in regolith and is made available for plant uptake. The results of Sect. 3.3 show that a substantial fraction of Mg once released by chemical weathering is taken up by plant and subsequently exported in Mg-containing CWD.

Biogeosciences Discuss., doi:10.5194/bg-2016-521, 2017
Manuscript under review for journal Biogeosciences
Published: 16 January 2017

4.6 Dissolved export fractions

To confirm that Mg is not the only element that is strongly bio-utilised, we compared the dissolved river flux (W^X_{diss}) with the net solubilisation flux (W^X_τ) by its ratio W^X_{diss}/W^X_τ for macronutrients (X) like K, Ca, P and the plant-beneficial element Si. This approach requires knowing the denudation rate D (Eq. (8)) from cosmogenic nuclides, and the discharge Q (Eq. (5)) from long-lasting gauging programs. Using directly the ratio W^X_{diss}/W^X_τ would be associated with large uncertainties because both methods integrate over entirely different time scales. To obtain a metric that is independent of D and Q, we normalised the fluxes W^X_{diss} and W^X_τ over their respective Na fluxes (Eq. (11)) and rearrange to the right-hand term of Eq. (11):

$$DEF^X = \frac{\frac{W^X_{diss}}{W^{Na}_{diss}}}{\frac{W^X_\tau}{W^{Na}_\tau}} = \frac{\left(\frac{[X]_{diss}}{[Na]_{diss}}\right)/\left(\frac{[X]_{rock}}{[Na]_{rock}}\right)}{\frac{(\tau^X_{Zr})}{(\tau^{Na}_{Zr})}}. \quad (11)$$

Na is the element of choice since it behaves conservatively, meaning Na is neither incorporated into secondary minerals nor taken up as a nutrient by plants. We call the Na-normalised ratio between W^X_{diss} and W^X_τ the dissolved export fraction (DEF^X, Eq. (11), Fig. 5). The DEF^X quantifies the dissolved riverine loss of X from the ecosystem relative to its net release from the regolith. At steady state, the DEF^X is less than 1 if some of the released element is partitioned into a plant uptake flux and then eroded as plant litter or CWD (including eroded phytoliths in the case of Si). If the DEF^X is larger than 1, other inputs are needed to explain the X mass balance, such as atmospheric deposition, for example.

The only case in which the Na normalisation may not fully remove time scale issues is, if, for example, changes in water flow during the development of the profile over a few thousand years result in non-steady dissolution of Na-bearing primary minerals relative to other primary minerals, or if the rate of secondary mineral formation changes relative to Na-bearing primary mineral decomposition. In that case the time-integrated denominator in Eq. (11) does not reflect the present value.

The DEF^X obtained (Fig. 5, Table S4d) show that of the elements solubilised from rock ~80 % of Ca, ~60 % of K, ~50 % of Si, ~40 % of Mg, and ~25 % of P appear in the streams dissolved load. The DEF for Mg is in excellent agreement with the 50-100 % of Mg bio-utilisation calculated independently by isotope mass balances (Eq. (2)). The high DEF for Ca is due to its high concentrations in rock combined with its high degree of solubilisation by chemical weathering that result in excess availability compared to the nutrient demand of trees. In contrast, the low DEF for P is due to its high biological demand and low availability, resulting in high degree of plant uptake and subsequent export in plant litter and CWD.

4.7 Nutrient recycling factor

After uptake and return to the forest floor, nutrients are not directly discharged into the stream by litter dissolution, or eroded as plant litter or CWD. Rather, they are subject to recycling - defined here as uptake of nutrients released from plant litter. Note that if nutrient uptake into plants equals nutrient return from plants, recycling does not change the stable isotope ratios

Biogeosciences Discuss., doi:10.5194/bg-2016-521, 2017
Manuscript under review for journal Biogeosciences
Published: 16 January 2017

of the involved compartments (Bouchez et al., 2013). In addition, the fluxes calculated above are net fluxes that do not take recycling into account. However, the recycling rate can be hypothesised to depend on the ratio of nutrient demand to availability. We thus tested the hypothesis that in our kinetically-limited setting, unlike in the supply-limited regime, intense nutrient recycling is not required as nutrient loss can be balanced by new uptake from regolith dissolution (Jobbagy and Jackson, 2001; Lucas, 2001). We quantified nutrient recycling as the number of passages an element X takes through the vegetation after its initial release from rock (quantified by the net solubilisation flux W_τ^X). We call this the elemental recycling factor (Rec^X). Rec^X is determined by Eq. (12) and reported in Table S4e:

$$Rec^X = \frac{L^X}{W_\tau^X}. \quad (12)$$

Because the nutrient uptake flux (U^X) is difficult to determine, we use the sum of litter fluxes (L^X) comprising foliage litter fall ($L^X_{foliage}$, Table S4c), root litter (L^X_{root}, Table S4c) and trunk litter (L^X_{trunk}, Table S4c) instead, assuming balanced uptake and litter fluxes. L^{Mg} is 16,000, 10,000 to 20,000, and 28,000 t km^{-2} yr^{-1} for foliage, stem, and root, respectively. L^X represents a minimum estimate for U^X and hence Rec^X is likely underestimated because we did not consider return of growth-limiting nutrients from foliage via phloem through roots back into soil during senescence and return of nutrients from throughfall or stem flow. Since litter data for Providence Creek is not available we use total foliage litter fall fluxes of *Pinus ponderosa* from literature (Grady and Hart, 2006; Klemmedson et al., 1990; Law et al., 1999) and multiply them with the elemental foliage litter concentration of *Pinus ponderosa* (Klemmedson et al., 1990) except for Si for which we used data from Bartoli (1983) to determine $L^X_{foliage}$. To determine L^X_{root} we used root litter production data from Röderstein et al. (2005) and since roots were not sampled in this study we used Mg, Ca and K root concentrations from *Picea abies* (Bolou-Bi et al., 2012), the P root concentration from *Pinus sylvestris* (George et al., 1997) and the Si *Pinus ponderosa* needle concentration from this study as elemental needle and root concentrations are generally similar and due to the lack of Si root concentration for coniferous trees in the literature. To determine L^X_{trunk} we estimated the *Pinus ponderosa* minimum and maximum trunk wood biomass by using an logging calculator (www.burleyboys.com, for input parameters see Appendix C) and *Pinus ponderosa* Mg, Ca, K and Si wood concentrations from this study and P wood concentration from *Pinus contorta* (Pearson et al., 1987).

At Providence Creek, we observe that P is the only bio-element that becomes enriched (Fig. 6) and tightly recycled in topsoil (Fig. 5). Although Rec^K is only slightly above unity we infer that K becomes also recycled since Rec^K is likely underestimated due to the lack of throughfall data which are generally highest for K compared to the other bio-elements (Boy and Wilcke, 2008). The Rec^X for the other bio-elements (Fig. 5) is low. The low Rec^X for the bio-elements but P is in agreement with our observation that after uptake the largest mass fraction of these bio-elements is disposed through export of plant litter and CWD. If nutrient supply from regolith were low, Rec^X would be high to satisfy ecosystem nutrition (Lang et al., 2016). At Providence Creek we observe a direct export pathway consistent with the kinetically-limited weathering regime of Providence Creek.

Biogeosciences Discuss., doi:10.5194/bg-2016-521, 2017
Manuscript under review for journal Biogeosciences
Published: 16 January 2017

4.8 Export mechanisms of bio-elements in coarse woody debris (CWD)

In the preceding sections, we have shown that bio-utilisation and solid export of CWD is required to explain the creek water being enriched in ^{24}Mg, and the deficit in the dissolved river export fraction indicated by the DEF^X. Here we discuss two CWD export mechanisms: a) logging on centennial time scales; and b) natural erosion in pre-anthropogenic times and over weathering (ky) time scales. Concerning logging, indeed in the late 19th century *Pinus ponderosa* forests became nearly wholesale clear-cut (Graham and Jain, 2005). These logging activities triggered the growth of today's forest at Providence Creek and might have shifted the ecosystem from steady state - where elemental input fluxes equal elemental export fluxes, and where plant growth equals plant mortality - into an ecosystem being in a transient state characterised by the build-up of a pool of bio-elements (e.g. Sommer et al., 2013). Concerning natural erosion, trunk wood that is enriched in ^{26}Mg is not contained in the sediment pond we sampled. Yet it is continuously removed from the ecosystem by stochastic events, such as landslides, tree turnover after tree death (Roering et al., 2010), wind throw, or frequent wildfires - that are suppressed since the late 19th century - after which ash is fast eroded.

To estimate whether tree trunk growth satisfies the elemental and isotopic mass balance we estimated the budgets of bio-elements contained in *Pinus ponderosa* trunk wood (see Sect. 3.8 and Appendix C). We find that the uptake fluxes (Table S4c) are indeed similar to the deficit in the elemental dissolved export fraction indicated by the DEF^X for Mg and Ca. Both the P and K trunk wood fluxes are higher than predicted by the DEF^X. This effect arises for strongly recycled elements, because the uptake flux contains the fraction added by nutrient recycling from the forest floor. However, the Si tree trunk budget is two orders of magnitudes lower than predicted by the DEF^{Si}. The reason is that for most tree species stem wood contains at least one order of magnitude lower Si concentrations than leaves (Cornelis et al. 2009). Thus, the low DEF of Si can be explained by Si export occurring in the bio-opal of phytoliths of which the dissolution half-life at the pH prevailing at Providence Creek amounts to a few 100 days (Fraysse et al., 2009).

Whether natural erosion of bio-elements by CWD is a feasible mechanism depends on whether the erosional time scale outcompetes the leaching time scale from CWD. Trunk wood decomposition fluxes have been quantified for *Fagus grandifolia*, *Acer saccharum* and *Betula alleghaniensis*. About 25-50 % of Ca, 30-70 % of P, 5-20 % of K, 20-40 % of Mg (Johnson et al. 2014), and 25-60 % of Si (Clymans et al., 2016) remain in trunk wood after 16 years of decomposition. For comparison, after 2 years of *Pinus ponderosa* foliage litter decomposition ~90% of Ca, ~55 % of P, ~20 % of K, ~45 % of Mg (Klemmedson, 1992) remain in foliage litter. Thus, bio-element leaching (except Ca) from foliage outpaces bio-element leaching from wood. Hence, after tree death and after litterfall (Si contained in phytoliths, and Ca likely contained in oxalates) erosional removal must occur within this decomposition time scales.

Biogeosciences Discuss., doi:10.5194/bg-2016-521, 2017
Manuscript under review for journal Biogeosciences
Published: 16 January 2017

Given the lack of information on the pre-logging fluxes and isotope ratios at Providence Creek we have no means to assess whether the natural CWD erosion mechanism has been in operation. We can speculate, however, that the export by logging is similar to the natural erosion of tree trunks in CWD as both are limited by tree growth. One other study, using stable Sr isotopes in an unperturbed ecosystem in New Zealand, shows a similar partitioning of Sr between plants and the river dissolved flux (Andrews et al, 2016). That data can be interpreted to imply natural erosion of Sr in plant litter and CWD. The same interpretation is possible for the data from the Shale Hills Critical Zone Observatory, where a similar deficit in heavy Mg isotopes was found in stream and soil water (Ma et al. 2015). In that study the bio-cycling hypothesis was dismissed on the grounds of missing accumulation of Mg in the organic rich portions of soil. The existence of a sub-micron pool enriched in ^{26}Mg was hypothesised instead. However, the Mg data would be compatible with the CWD export hypothesis.

4.9 Nutrient uplift from the deep saprolite

Finally, we determine the depth from which these nutrients are uplifted. A first indicator is the depth distribution of loss fractions τ^X (Brantley and Lebedeva, 2011) that allows for the identification of so-called biogenic profiles that are characteristically depleted at depth and become enriched in topsoil, because nutrients are uplifted from depth (Jobbagy and Jackson, 2001; Lucas, 2001). Whereas P depletion amounts to 85 % at 3 m depth and increases towards the surface indicating biogenic uplift of P, the loss fractions of Mg, K, and Si amount to 20 to 40 % and show uniform depletion along the entire depth of the weathering zone down to 7 m depth. The traditional view is that this loss is induced by mineral dissolution and removal by infiltrating water (Brantley and Lebedeva, 2011). We can use Mg isotopes to explore an alternative hypothesis: that these nutrients are taken up by tree roots or associated mycrorrhiza fungi (Jongmans et al., 1997; Landeweert et al., 2001; Lucas, 2001) at these deep levels. In the absence of Mg-clays and carbonates the isotopically light composition of the exchangeable fraction throughout the regolith ($\delta^{26}Mg_{exch}$, Fig. 3) can only be caused by the preferential uptake of heavy Mg isotopes by trees. We can exclude that the development of such an isotopically light exchangeable Mg compartment throughout the regolith is due to fractionation during adsorption (Opfergelt et al., 2014) as the associated fractionation factor is close to 0 ‰ (Wimpenny et al., 2014). We can also exclude that low $\delta^{26}Mg_{soil\ water}$ infiltrates to depth from the surface as this $\delta^{26}Mg_{soil\ water}$ would be masked by the high Mg solubilisation flux from primary minerals (Fig. 4). Deep water uptake from down to 7 m is supported by the rooting depth of *Pinus ponderosa* which can reach up to 24 m (Stone and Kalisz, 1991).

5 Implications

To date the possible acceleration of weathering by plants has only been inferred indirectly, by comparing the flux of watersheds of different vegetation cover over short time scales (Moulton et al., 2000). At Providence Creek a substantial fraction of bio-elements released by rock dissolution over typical weathering time scales (thousands of years) is directly utilised by the local forest trees - where nutrient uptake does not depend on the mechanism of export. Our data provide the first direct observation of the role biota plays in contributing to weathering fluxes in a given ecosystem. The partitioning of Sr stable isotopes in a

Biogeosciences Discuss., doi:10.5194/bg-2016-521, 2017
Manuscript under review for journal Biogeosciences
Published: 16 January 2017

mountain catchment in New Zealand (Andrews et al., 2016) can be interpreted in the same way. It is essential to both metal isotope-based observations that the bio-elements taken up are directly exported in CWD. The low recycling factors observed support this notion of rapid nutrient uptake and disposal. Therefore, in this kinetically-limited setting, weathering up to 7 m depth is tightly coupled to nutrient utilisation and erosion. We do not know whether this deep nutrient uptake is actively driven by nutrient demand (Brantley et al., 2011; Landeweert et al., 2001; Lucas, 2001), or is coupled to deep water uptake during summer droughts. Regardless, either cause would deepen the weathering advance front and potentially facilitates the balance between erosion and weathering advance rate (Brantley et al., 2011).

Considering that 30 % of the Earth's surface is covered by forests (Bonan, 2008) the export of the utilised bio-elements in CWD and bio-opal might represent a more widespread phenomenon. Indeed, in active mountain belts the weathering intensity (total chemical weathering rate normalised by denudation rate) derived from river loads is far lower than that derived from regolith (Dixon and von Blanckenburg, 2012). We suggest that one possible explanation for this discrepancy is the nutrient uptake by biota and its subsequent erosion as bio-opal, leaf litter, and CWD in these predominantly kinetically-limited weathering regimes. In contrast, in lowland supply-limited regimes and floodplains the low bio-element concentrations in plant debris, the low particulate organic matter sediment yield (0.1-1 % of total sediment yield) (Galy et al., 2015) and the low amorphous opal flux (0.6 % of total sediment yield) (Frings et al., 2016) results in nutrient export to occur predominantly in the dissolved form. The postulated fast weathering and rapid nutrient erosion coupling is significant only in geologically active mountains where CWD and bio-opal erosion is high (Galy et al., 2015; McCorkle et al., 2016), outpaces nutrient recycling, and might constitute a significant solid export flux of elements released by weathering and hence not accounted for in weathering flux estimates based on dissolved river loads.

6 Conclusions

The Mg isotope composition of stream water in Providence creek, Southern Sierra Nevada, requires a compartment separation between isotopically light Mg dissolved in water and isotopically heavy Mg exported in tree wood, without substantial re-mineralization and re-utilisation. A steady state isotope mass balance supports the solid Mg export path in that the Mg export is dominated by particulates, and only a minor fraction of ~14 % of Mg is exported as solutes. Thus 50-100 % of Mg that is released from primary minerals is utilised by trees. This high Mg bio-utilisation is confirmed by a deficit apparent in the Na-normalised dissolved river Mg export flux when compared to the Na-normalised net Mg solubilisation flux. The deficit of dissolved Mg, exported by creeks, amounts to 60 %, meaning that 60 % of Mg is bio-utilised. We find similar deficits amounting to ~40 % for K, ~20 % for Ca, ~50 % for Si and ~75 % for P. These three lines of evidence show that weathering of rock and biogenic uptake are tightly coupled in this fast weathering, kinetically-limited regime. In support of this rock-derived nutrient supply scenario we find that no bio-element except P becomes substantially re-mineralised and re-utilised by recycling from organic litter. Instead, we infer that Mg and other bio-elements are disposed from the forest ecosystem in coarse

Biogeosciences Discuss., doi:10.5194/bg-2016-521, 2017
Manuscript under review for journal Biogeosciences
Published: 16 January 2017

woody debris (CWD) and Si in phytoliths eroded with leaf litter. Today CWD is exported by logging. In pre-anthropogenic times, the same CWD has potentially been eroded following tree death, during landslides, or after wind throw. We find that Mg is taken up from trees along the entire depth of the weathering profile down to 7 m depth as indicated by the light Mg isotopic composition of the easily exchangeable soil fraction. Therefore we provide the first direct observation that biota actively affects weathering fluxes. We conclude that in this kinetically-limited regime weathering is tightly coupled to rapid nutrient utilisation and erosion. Finally, we speculate that rapid nutrient erosion might be coupled to fast weathering globally. This coupling then is significant in geologically active mountains where CWD and bio-opal erosion is high and might present a hitherto underestimated solid export flux of elements previously released by weathering.

7 Appendices

Appendix A: Calculating δ^{26}Mg in bulk tree

We calculate the Mg isotopic composition of bulk tree ($\delta^{26}Mg_{tree}$) by a mass balance comprising the above-ground (needles, branches, stem) and belowground (roots) tree compartments. We measured δ^{26}Mg in foliage and stem wood. To estimate the isotopic composition of bulk *Pinus ponderosa* and *Pinus jeffrey* we combine these results with δ^{26}Mg and Mg concentration from (Bolou-Bi et al., 2012) and the biomass of different compartments of *Pinus ponderosa* from (Laclau, 2003). We did not measure δ^{26}Mg in roots because of the challenges related to their purification from soil particles. Instead we use the published difference between δ^{26}Mg in roots and δ^{26}Mg in wood (Bolou-Bi et al., 2012) to infer δ^{26}Mg in roots from our measured value in wood. The isotopic composition of bulk tree is finally calculated by Eq. (A1), where $f^{Mg}_{compartment}$ is the fraction of Mg in a given tree compartment.

$$\delta^{26}Mg_{bulk\,tree} = f^{Mg}_{needle} \cdot \delta^{26}Mg_{needle} + f^{Mg}_{stem} \cdot \delta^{26}Mg_{stem} + f^{Mg}_{root} \cdot \delta^{26}Mg_{root} \quad \text{(A1)}$$

The inferred isotopic composition of roots is 0.43 ‰ for *Pinus ponderosa* and 0.34 ‰ for *Pinus jeffrey*. The $\delta^{26}Mg_{tree}$ plotted in Fig. 3 represents a mean value of bulk *Pinus ponderosa* and *Pinus jeffrey*.

Appendix B: X-ray diffraction analyses and the potential incorporation of Mg into secondary minerals

Powder X-ray diffraction analyses (Siemens D5000, Cu-Kα radiation) were performed for mineral identification on selected soil, saprolite and bedrock samples. Figure B1 indicates characteristic reflections for some major and minor minerals. Kaolinite is the only secondary mineral identified. The limit of detection is 5 %.

The absence of Mg-clays and the presence of kaolinite was confirmed by a published clay content of less than 10 % in the soils (Dahlgren et al., 1997), and by thermodynamic modelling (PhreeqC). Because kaolinite has a low Mg content (<0.03 wt%) (Wimpenny et al., 2014) and a relatively low adsorption cation exchange capacity (CEC) of < 10 $cmol_c\ kg^{-1}$ (Wimpenny

Biogeosciences Discuss., doi:10.5194/bg-2016-521, 2017
Manuscript under review for journal Biogeosciences
Published: 16 January 2017

et al., 2014) it is unlikely to incorporate Mg in such amounts that the Mg mass balance in soil is affected. Therefore, neoformation of Mg-clays is not the mechanism that preferentially removes ^{26}Mg from soil solution.

The fraction of Mg potentially contained in clay (f_{sec}^{Mg}) was calculated from the following mass balance. f_{sec}^{Mg} is governed by a mixture between Mg partitioned into Mg-clays and Mg partitioned into primary minerals such as biotite and amphibole. While the abundances of Mg-clays is at maximum 5 % (XRD limit of detection), primary minerals like biotite and amphibole are identified but not quantified by XRD. Hence, we estimate the relative abundances of biotite and amphibole from bedrock analysis (Bateman and Wones, 1972) which we consider to be applicable to soil too given the kinetically-limited weathering regime. We assume all mafic constituents to contain Mg. We use montmorillonite $(Al_{1.67}Mg_{0.33})[(OH)_2Si_4O_{10}]Na_{0.33}{*}H_2O$ (Harder, 1972) and biotite $K(Mg)_3[(OH,Fe)_2(Al,Fe,Ti)Si_3O_{10}]$ as model endmembers for Mg-clays and Mg carrying primary minerals, respectively. Applying the mineral Mg stoichiometry to the abundances of Mg-clays and biotite reveals that a Mg-clay content of 5 % in the soil translates into 4 % Mg partitioned into Mg-clays and 96 % Mg partitioned into biotite. This 4 % is used for f_{sec}^{Mg} in Eq. (1), which is solved for $\delta^{26}Mg_{sec}$ (see Sect. 3.2).

This calculation confirms that the bulk soil sample with the highest measured $\delta^{26}Mg$ (-0.05 ‰), assuming it contains a maximum allowable Mg-clay content of 5 %, can only be explained if $\delta^{26}Mg_{sec}$ is +4.0 ‰, which is highly unlikely (Wimpenny et al., 2014 and references therein). Alternatively, if we use the maximum $\delta^{26}Mg_{sec}$ value observed for Mg-clay of 0.5 ‰ (Ryu et al., 2016 and references therein) in Eq. (1), then the Mg fraction in the bulk soil carried by Mg-clays (f_{sec}^{Mg}) were 24 %. This 24 % Mg partitioned into Mg-clays can be converted into a 30 % Mg-clay content in the bulk soil, which by far exceeds the XRD detection limit. Such high clay content was not observed by XRD (Fig. B1).

Finally, we explore whether Mg isotope fractionation by Mg adsorption onto kaolinite and amorphous hydroxides might result in the negative $\delta^{26}Mg_{diss}$. The evidence for Mg isotope fractionation during adsorption/desorption is not conclusive and is discussed in (Wimpenny et al., 2014 and references therein). Recent experimental evidence suggests that Mg adsorption is mostly associated with a slightly negative (-0.1 ‰) or complete absence of Mg isotope fractionation. Thus, our adsorbed Mg (termed 'exchangeable') likely reflects the isotopic composition of the fluid from which the exchange occurred. Indeed our isotopically light exchangeable Mg isotope analyses is virtually identically to $\delta^{26}Mg_{diss}$.

Moreover, for such a process to shift $\delta^{26}Mg$ in the isotope mass balance (Eq. (1)), a substantial amount of Mg would need to be adsorbed. Our analyses of exchangeable Mg mass in regolith samples indicate that this compartment makes up less than 0.52 % of the bulk regolith sample (Table S1). This low mass is consistent with the low cation exchange capacity measured in Providence Creek soils (e.g., $Mg^{2+} < 0.45$ $cmol_c$ kg^{-1}, Johnson et al., 2011). Hence, neither clay formation nor adsorption is the mechanism that removes isotopically heavy Mg from soil solutions.

Biogeosciences Discuss., doi:10.5194/bg-2016-521, 2017
Manuscript under review for journal Biogeosciences
Published: 16 January 2017

Appendix C: Input data to estimate *Pinus ponderosa* trunk wood biomass

To estimate a lower limit of *Pinus ponderosa* trunk wood biomass, we use a diameter at breast height (DBH) of 63 cm (Law et al., 1999), an upper diameter of 42 cm (by assuming that the diameter in the crown is reduced by one third compared to the DBH), a tree height of 34 m (Law et al., 1999), and a stand density of 40,000 trees per square kilometre. To convert the trunk wood biomass into an annual growing flux we used a living time of 250 years (Law et al., 1999). To estimate an upper limit of *Pinus ponderosa* trunk wood biomass we assume a younger forest (200 years) but denser (62,500 trees per square kilometre) forest stand.

8 Author contributions

D.U. analysed samples, interpreted data, wrote text. J.S. conducted field work, analysed samples, interpreted data, wrote text. J.B. conducted field work, interpreted data, wrote text. J.D. conducted field work, provided background information. F.v.B. designed study, conducted field work, interpreted data, wrote text.

9 Competing financial interests

The authors declare no competing financial interests.

10 Additional information

Supplementary data tables are available in the online version of the paper.

11 Acknowledgements

We thank R. Naumann (GFZ) for X-ray diffraction and X-ray fluorescence analyses. A. Gottsche (GFZ) is acknowledged for anion quantification using ion chromatography and for assistance in X-ray fluorescence analyses. We also thank R. Meyer (GFZ) for trace element water analyses by ICP-MS (iCAP-Q). Logistical support and discharge data was provided by the NSF-supported Southern Sierra Critical Zone Observatory: time-series water sampling, sample pre-treatment and shipping was done by M. Meadows (University of California, Merced); C. Hunsacker (US Forest Service, Fresno) is thanked for field support and daily Providence Creek discharge data (http://criticalzone.org/sierra/data). We thank M. Oelze (GFZ), F. Lang (University of Freiburg) and W. Wilcke (KIT, Karlsruhe) for discussions. D.U. and F.v.B. are grateful for funding by the German National Science Foundation priority Program 1685 “Ecosystem nutrition: forest strategies for limited phosphorus resources”.

Biogeosciences Discuss., doi:10.5194/bg-2016-521, 2017
Manuscript under review for journal Biogeosciences
Published: 16 January 2017

12 References

Andrews, M. G., Jacobson, A. D., Lehn, G. O., Horton, T. W., and Craw, D.: Radiogenic and stable Sr isotope ratios (87Sr/86Sr, δ88/86Sr) as tracers of riverine cation sources and biogeochemical cycling in the Milford Sound region of Fiordland, New Zealand, Geochim. Cosmochim. Ac., 173, 284-303, 2016.

Arunachalam, J., Emons, H., Krasnodebska, H. and Mohl, C.: Sequential extraction studies on homogenized forest soil samples, Sci. Total Environ., 181, 147-159, 1996.

Bales, R. C., Hopmans, J. W., O'Geen, A. T., Meadows, M., Hartsough, P. C., Kirchner, P., Hunsaker, C. T. and Beaudette, D.: Soil moisture response to snowmelt and rainfall in a Sierra Nevada Mixed-Conifer forest, Vadose Zone J., 10, 786-799, 2011.

Bartoli, F.: The biogeochemical cycle of silicon in two temperate forest ecosystems, Ecol. Bull., 35, 469-476, 1983.

Bateman, P.C. and Wones, D.R.: Huntington Lake Quadrangle, Central Sierra Nevada, California - Analytical Data, Shorter Contributions to General Geology, Geological Survey Professional Paper 724-A, 1972.

Black, J. R., Epstein, E., Rains, W. D., Yin, Q.-Z. and Casey, W. H.: Magnesium-isotope fractionation during plant growth, Environ. Sci. Technol., 42, 7831-7836, 2008.

Bolou-Bi E.B., Poszwa, A., Leyval, C. and Vigier, N.: Experimental determination of magnesium isotope fractionation during higher plant growth, Geochim. Cosmochim. Acta., 74, 2523-2537, 2010.

Bolou-Bi, E. B., Vigier, N., Poszwa, A., Boudot, J. P., and Dambrine, E.: Effects of biogeochemical processes on magnesium isotope variations in a forested catchment in the Vosges Mountains (France), Geochim. et Cosmochim. Acta, 87, 341-355, 2012.

Bonan, G.B.: Forests and climate change: forcings, feedbacks, and the climate benefits of forests, Science, 320, 1444-1449, 2008.

Bouchez, J., von Blanckenburg, F. and Schuessler, J. A.: Modelling novel stable isotopes in the weathering zone, Am. J. Sci., 313, 267-308, 2013.

Boy, J., and Wilcke, W.: Tropical Andean forest derives calcium and magnesium from Saharan dust, Global Biogeochem. Cy., 22, 2008.

Brantley, S. L. and Lebedeva, M.: Learning to Read the Chemistry of Regolith to Understand the Critical Zone, Annu. Rev. Earth Pl. Sc., 39, 387-416, 2011.

Brantley, S. L., Megonigal, J. P., Scatena, F. N., Balogh-Brunstad, Z., Barnes, R. T., Bruns, M. A., Van Cappellen, P., Dontsova, K., Hartnett, H. E., Hartshorn, A. S., Heimsath, A., Herndon, E., Jin, L., Keller, C. K., Leake, J . R., McDowell, W. H., Meinzer, F. C., Mozdzer, T. J ., Petsch, S., Pett-Ridge, J., Pregitzer, K. S., Raymond, P. A., Riebe, C. S., Shumaker, K., Sutton-Grier, A., Walter, R. and Yoo, K.: Twelve testable hypotheses on the geobiology of weathering, Geobiology, 9, 1-26, 2011.

Burley Boys: http://www.burleyboys.com, last access: 23th November 2016

Chapela Lara, M., Buss, H. L., Pogge von Strandmann, P. A. E., Moore, O. W. and Schuessler, J. A.: The influence of critical zone processes on the Mg isotope budget in a tropical, highly weathered andesitic catchment, Geochim. Cosmoch.f Ac., 2016, in revision.

Clymans, W., Conley, D. J., Battles, J. J., Frings, P. J., Koppers, M. M., Likens, G. E., and Johnson, C. E.: Silica uptake and release in live and decaying biomass in a northern hardwood forest, Ecology, 97, 3044-3057, 2016.

Cornelis, J. T., Ranger, J., Iserentant, A., and Delvaux, B.: Tree species impact the terrestrial cycle of silicon through various uptake, Biogeochemistry, 97, 231-245, 2010.

Critical Zone: http://criticalzone.org/sierra/data/datasets, last access: 15th November 2016

Dahlgren, R. A., Boettinger, J. L., Huntington, G. L. and Amundson, R. G.: Soil development along an elevational transect in the western Sierra Nevada, California, Geoderma, 78, 207-236, 1997.

Dixon, J. L., Heimsath, A. M. and Amundson, R.: The critical role of climate and saprolite weathering in landscape evolution, Earth Surf. Proc. Land., 34, 1507-1521, 2009.

Dixon. J. L. and von Blanckenburg, F.: Soils as pacemakers and limiters of global silicate weathering, C. R. Geosci., 344, 597-609, 2012.

Eagan, S. M., Hunsaker, C. T., Dolanc, C. R., Lynch, M. E. and Johnson, C. R.: Discharge and Sediment Loads at the Kings River Experimental Forest in the Southern Sierra Nevada of California, 2007.

Fantle, M. S. and Tipper, E. T.: Calcium isotopes in the global biogeochemical Ca cycle: Implications for development of a Ca isotope proxy, Earth Sci. Rev., 129, 148–177, 2014.

Fraysse, F., Pokrovsky, O. S., Schott, J. and Meunier, J.-D.: Surface chemistry and reactivity of plant phytoliths in aqueous solutions, Chem. Geol., 258, 197-206, 2009.

Frings, P. J., Clymans, W., Fontorbe, G., De La Rocha, C. L. and Conley, D. J.: The continental Si cycle and its impact on the ocean Si isotope budget, Chem.Geol., 425, 12-36, 2016.

Galy, A., Yoffe, O., Janney, P. E., Williams, R. W., Cloquet, C., Alard, O., Halicz, L., Wadhwa, M., Hutcheon, I. D., Ramon, E. and Carignan, J.: Magnesium isotope heterogeneity of the isotopic standard SRM980 and new reference materials for magnesium-isotope-ratio measurements, J. Anal. At. Spectrom., 18, 1352–1356, 2003.

Galy, V., Peucker-Ehrenbrink, B. and Eglington, T.: Global carbon export from the terrestrial biosphere controlled by erosion, Nature, 521, 204-207, 2015.

George, E., Seith, B., Schaeffer, C., and Marschner, H.: Responses of Picea, Pinus and Pseudotsuga roots to heterogeneous nutrient distribution in soil, Tree Physiol., 17, 39-45, 1997.

Grady, K. C. and Hart, S. C.: Influences of thinning, prescribed burning, and wildfire on soil processes and properties in southwestern ponderosa pine forests: a retrospective study, For. Ecol. Manag., 234, 123-135, 2006.

Graham, R. T. and Jain, T. B.: Ponderosa Pine Ecosystems, USDA Forest Service Gen. Tech. Rep., PSW-GTR-198, 2005.

Hahm, W. J., Riebe, C. S., Lukens, C. E. and Araki, S.: Bedrock composition regulates mountain ecosystems, P. Natl. Acad. Sci. USA, 111, 3338-3343, 2014.

Harder, H.: The role of magnesium in the formation of smectite mineral,. Chem. Geol, 10, 31-39, 1972.

Jobbagy, E. G. and Jackson R.B.: The distribution of soil nutrients with depth: Global patterns and the imprint of plants, Biogeochemistry, 53, 51-77, 2001.

Johnson, C. M., Beard, B. L. and Albarède, F.: Geochemistry of Non-Traditional Stable Isotopes, Rev. Mineral. Geochem., 55, 2004.

Johnson, C. E., Siccama, T. G., Denny, E. G., Koppers, M. M. and Vogt, D. J.: In situ decomposition of northern hardwood tree boles: decay rates and nutrient dynamics in wood and bark, Can. J. Forest Res., 44, 1515-1524, 2014.

Johnson, D.W., Hunsaker, C.T., Glass , D.W., Rau, B.M. and Roath, B.A.: Carbon and nutrient contents in soils from the Kings River Experimental Watersheds, Sierra Nevada Mountains, California, Geoderma, 160, 490-502, 2011.

Jongmans, A.G., van Breemen, N., Lundström, U., van Hees, P. A. W., Finlay, R. D., Srinivasan, M., Unestam, T., Giesler, R., Melkerud, P.-A. and Olsson, M.: Rock-eating fungi, Nature, 389, 682-683, 1997.

Klemmedson, J. O., Meier, C. E. and Campbell, R. E.: Litter fall transfers of dry matter and nutrients in ponderosa pine stands, Can. J. Forest Res., 20, 1105-1115, 1990.

Klemmedson, J. O.: Decomposition and nutrient release from mixtures of Gambel oak and ponderosa pine leaf litter, Forest Ecol. Manag., 47, 349-361, 1992.

Laclau, P.: Biomass and carbon sequestration of ponderosa pine plantations and native cypress forests in northwest Patagonia, Forest Ecol. Manag., 180, 317-333, 2003.

Landeweert, R., Hoffland, E., Finlay, R. D., Kuyper, T. W. and van Breemen, N.: Linking plants to rocks: ectomycorrhizal fungi mobilize nutrients from minerals, TRENDS Ecol. Evol., 16, 248-254, 2001.

Lang, F., Bauhus, J., Frossard, E., George, E., Kaiser, K., Kaupenjohann, M., Krüger, J., Matzner, E., Polle, A., Prietzel, J., Rennenberg, H. and Wellbrock, N.: Phosphorus in forest ecosystems: New insights from an ecosystem nutrition perspective, J. Plant Nutr. Soil Sc., 179, 129-135, 2016.

Law, B. E., Ryan, M. G. and Anthoni, P. M.: Seasonal and annual respiration of a ponderosa pine ecosystem, Glob. Change Biol., 5, 169-182, 1999.

Lucas, Y.: The role of plants in controlling rates and products of weathering: Importance of biological pumping, Annu. Rev. Earth Pl. Sc., 29, 135-163, 2001.

Ma, L., Teng, F. Z., Jin, L., Ke, S., Yang, W., Gu, H. O. and Brantley, S. L.: Magnesium isotope fractionation during shale weathering in the Shale Hills Critical Zone Observatory: Accumulation of light Mg isotopes in soils by clay mineral transformation, Chem. Geol., 397, 37-50, 2015.

Mahowald, N. M., Baker, A.R., Bergametti, G., Brooks, N., Duce, R.A., Jickells, T.D., Kubilay, N., Prospero, J.M., and Tegen, I. Atmospheric global dust cycle and iron inputs to the ocean. Global Biogeochemical Cycles, 19, 2005.

Mavromatis, V., Prokushkin, A. S., Pokrovsky, O. S., Viers, J. and Korets, M. A.: Magnesium isotopes in permafrost-dominated Central Siberian larch forest watersheds, Geochim. Cosmochim. Ac., 147, 76-89, 2014.

McCorkle, E. M., Berhe, A. A., Hunsaker, C. T., Johnson, D. W., McFarlane, K. J., Fogel, M. L. and Hart, S. C.: Tracing the source of soil organic matter eroded from temperate forest catchments using carbon and nitrogen isotopes, Chem. Geol., 44, 172-184, 2016.

Meng-Ning, D. A. I., Zhi-An, B. A. O., Kai-Yun, C. H. E. N., and Hong-Lin, Y. U. A. N.: In situ Analysis of Mg Isotopic Compositions of Basalt Glasses by Femtosecond Laser Ablation Multi-collector Inductively Coupled Plasma Mass Spectrometry, Chinese J. Anal. Chem., 44, 173-178, 2016.

Moulton, K. L., West, J. and Berner, R. A.: Solute flux and mineral mass balance approaches to the quantification of plant effects on silicate weathering, Am. J. Sci., 300, 539–570, 2000.

Oeser, M., Wexer, S., Horn, I., and Schuth, S.: High-Precision Fe and Mg Isotope Ratios of Silicate Reference Glasses Determined In Situ by Femtosecond LA-MC-ICP-MS and by Solution Nebulisation MC-ICP-MS, Geostand. Geoanal. Res., 38, 311-328, 2014.

Opfergelt, S. and Delmelle, P.: Silicon isotopes and continental weathering processes: Assessing controls on Si transfer to the ocean, C. R. Geosci., 344, 723-738, 2012.

Opfergelt, S., Burton, K.W., Georg, R.B., West, A.J., Guicharnaud, R.A., Sigfusson, B., Siebert, C., Gislason, S.R. and Halliday, A.N.: Magnesium retention on the soil exchange complex controlling Mg isotope variations in soils, soil solutions and vegetation in volcanic soils, Iceland, Geochim. Cosmochim. Ac., 125, 110-130, 2014.

Pearson, J. A., Knight, D. H., and Fahey, T. J.: Biomass and nutrient accumulation during stand development in Wyoming lodgepole pine forests, Ecology, 68, 1966-1973, 1987.

Pogge von Strandmann, P.A.E., Elliott, T., Marschall, H. R., Coath, C., Lai, Y.-J., Jeffcoate, A. B. and Ionov, D. A.: Variations of Li and Mg isotope ratios in bulk chondrites and mantle xenoliths. Geochim. Cosmochim. Ac., 75, 5247-5268, 2011.

Porder, S., Vitousek, P. M., Chadwick, O. A., Chamberlain, C. P. and Hilley, G. E.: Uplift, Erosion and Phosphorus Limitation in Terrestrial Ecosystems, Ecosystems, 10, 158-170, 2007.

Riebe, C.S., Kirchner, J.W. and Finkel, R.C.: Long-term rates of chemical weathering and physical erosion from cosmogenic nuclides and geochemical mass balance, Geochim. Cosmochim. Ac., 67, 4411-4427, 2003.

Riebe, C. S. and Granger, D. E.: Quantifying effects of deep and near-surface chemical erosion on cosmogenic nuclides in soils, saprolite, and sediment, Earth Surf. Proc. Land., 38, 523-533, 2013.

Röderstein, M., Hertel, D. and Leuschner, C.: Above-and below-ground litter production in three tropical montane forests in southern Ecuador, J. Trop. Ecol., 21, 483-492, 2005.

Roering, J. J., Marshall, J., Booth, A. M., Mort, M. and Jin, Q. S.: Evidence for biotic controls on topography and soil production, Earth Planet. Sc. Lett., 298, 183-190, 2010.

Ryu, J.-S., Vigier, N., Decarreau, A., Lee, S.-W., Le, K.-S., Song, H. and Petit, S.: Experimental investigation of Mg isotope fractionation during mineral dissolution and clay formation, Chem. Geol., 445, 135-145, 2016.

Schuessler, J. A., and von Blanckenburg, F.: Testing the limits of micro-scale analyses of Si stable isotopes by femtosecond laser ablation multicollector inductively coupled plasma mass spectrometry with application to rock weathering, Spectrochim. Acta B, 98, 1-18, 2014.

Schuessler, J. A., Kämpf, H., Koch, U., Alawi, M.: Earthquake impact on iron isotope signatures recorded in mineral spring water. Journal of Geophysical Research: Solid Earth, 121, 2016. doi:10.1002/2016JB013408

Sommer, M., Jochheim, H., Höhn, A., Breuer, J., Zagorski, Z., Busse, J., and Kaczorek, D.: Si cycling in a forest biogeosystem–the importance of transient state biogenic Si pools, Biogeosciences, 10, 4991-5007, 2013.

Stone, E. L. and Kalisz, P. J.: On the maximum extent of tree roots, For. Ecol. Manag., 46, 59-102, 1991.

Tipper, E.T., Lemarchand, E., Hindshaw, R.S., Reynolds, B.C. and Bourdon, B.: Seasonal sensitivity of weathering processes: hints from magnesium isotopes in a glacial stream, Chem. Geol., 312-313, 80-92, 2012.

Vitousek, P. M. and Farington, H.: Nutrient limitation and soil development: Experimental test of a biogeochemical theory, Biogeochemistry, 37, 63-75, 1997.

Wang, K., and Jacobsen, S. B.: An estimate of the Bulk Silicate Earth potassium isotopic composition based on MC-ICPMS measurements of basalts, Geochim. Cosmochim. Ac., 178, 223-232, 2016.

West, A.J., Galy, A. and Bickle, M.J.: Tectonic and climatic controls on silicate weathering, Earth Planet. Sc. Lett., 235, 211-228, 2005.

Wimpenny, J., Colla, C. A., Yin, Q.-Z., Rustad, J. R. and Casey, W. H.: Investigating the behavior of Mg isotopes during the formation of clay minerals, Geochim. Cosmochim. Ac., 128, 178-194, 2014.

Biogeosciences Discuss., doi:10.5194/bg-2016-521, 2017
Manuscript under review for journal Biogeosciences
Published: 16 January 2017

13 Figures

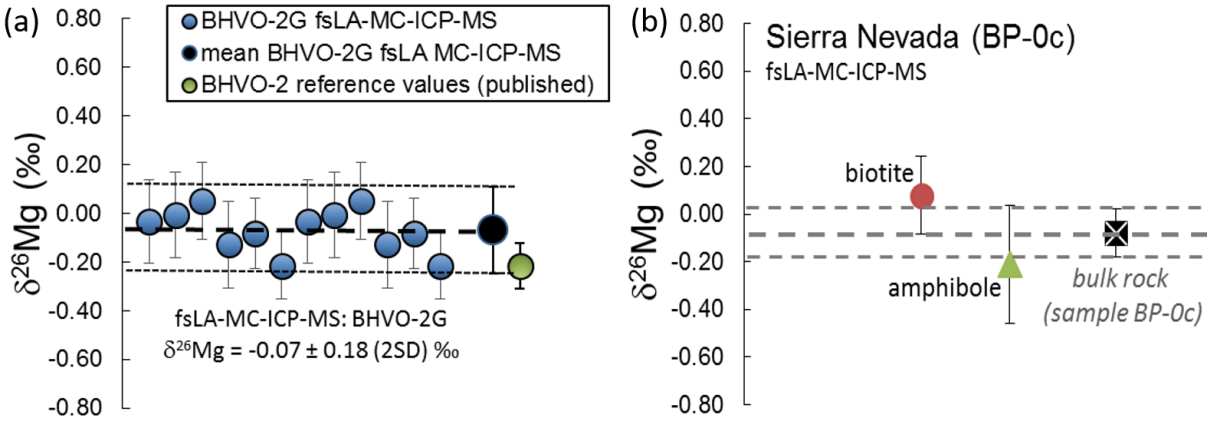

Fig. 1: Mg isotopic composition measured by fsLA-MC-ICP-MS. *(a): Repeat measurements of BHVO-2G. Solid black circle and bold dashed line repesents mean value of all BHVO-2G measurements with the 2SD range resprented by stippled lines. Published literature data (Meng-Ning et al., 2016) is shown for comparison. (b): Biotite and amphibole of sample BP-0c measured by fsLA-MC-ICP-MS. Bulk rock is measured by solution MC-ICP-MS.*

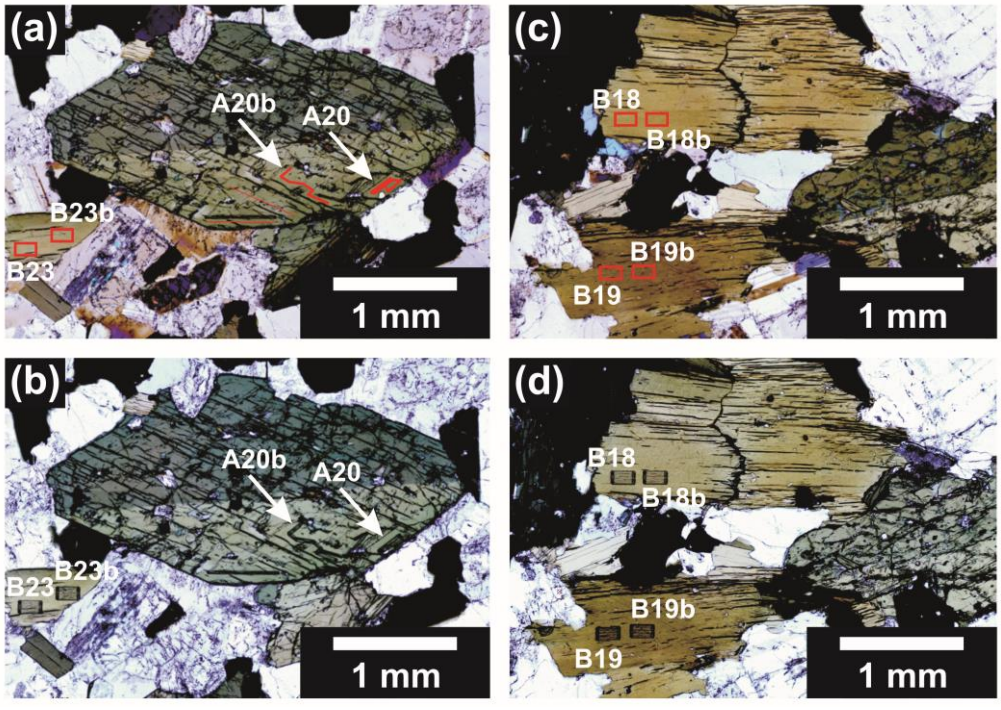

Fig. 2: Photomicrographs before and after fsLA-MC-ICP-MS. *Red rectangles and lines indicate laser ablation locations. Amphibole before (a) and after (b) fsLA-MC-ICP-MS. Biotite before (c) and after (d) fsLA-MC-ICP-MS.*

Biogeosciences Discuss., doi:10.5194/bg-2016-521, 2017
Manuscript under review for journal Biogeosciences
Published: 16 January 2017

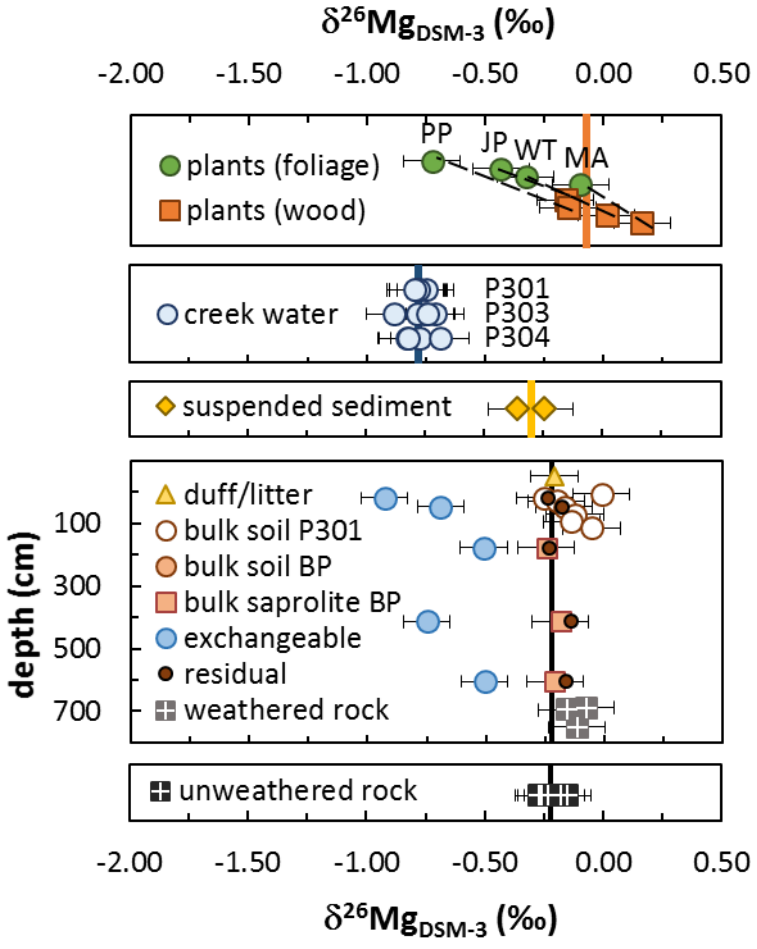

695

Fig. 3: Magnesium isotopic composition of the compartments at Providence Creek, Southern Sierra Nevada, USA. *Vertical lines represent mean δ^{26}Mg values of bulk unweathered rock (black), bulk suspended sediment (yellow), bulk tree (orange, mass balance see Appendix C), and creek water (blue). The diagonal stippled lines connect woody with non-woody plant material of the same sample. Exchangeable and residual: sequentially extracted soil phases; P301, P303, P304: headwater catchments at Providence Creek; BP: soil-saprolite profile (Balsam Profile); PP: Ponderosa Pine [Pinus ponderosa]; JP: Jeffrey Pine [Pinus jeffreyi]; WT: Whitethorn [Ceanothus cordulatus]; MA: Manzanita [Arctostaphylos manzanita]. Error bars: 0.10 ‰ (2SD).*

700

Biogeosciences Discuss., doi:10.5194/bg-2016-521, 2017
Manuscript under review for journal Biogeosciences
Published: 16 January 2017

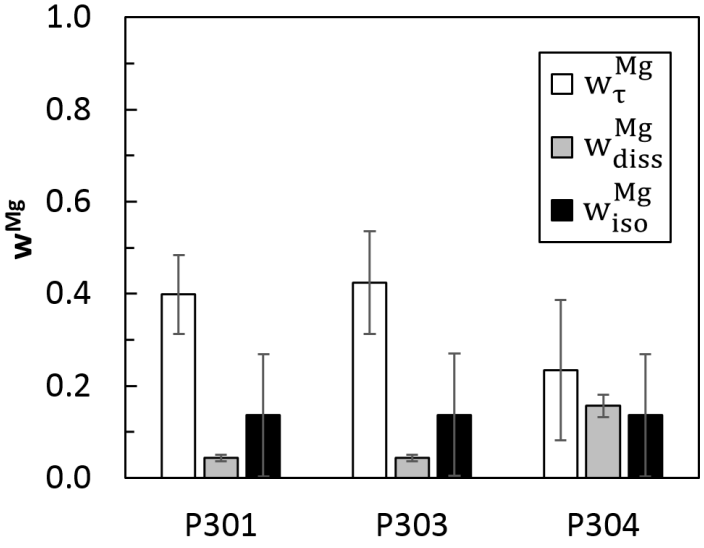

Fig. 4: Comparison of the relative weathering flux derived from Mg isotopes (w_{iso}^{Mg}, Table S4b), dissolved river loads (w_{diss}^{Mg}, Table S4b), and net solubilisation fluxes (w_{τ}^{Mg}, Table S4b) for the individual Providence Creek sub-catchments. *The ca. fourfold higher w_{diss}^{Mg} of the smallest watershed P304 compared to the larger watersheds P301 and P303 might be the result of the relatively high discharge record caused by higher baseflow (Eagan et al., 2007) for such a small watershed. For that reason we consider this catchment to be unrepresentative.*

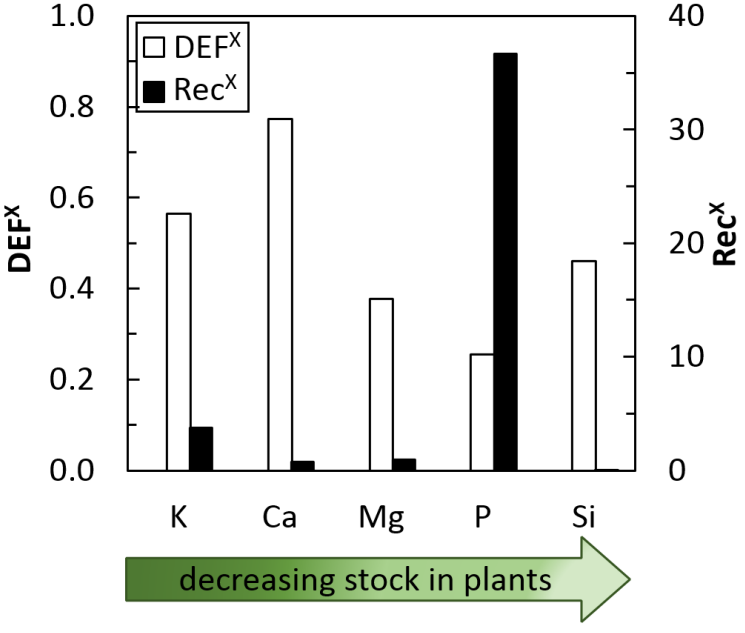

Fig. 5: Dissolved export fraction (DEF^X, left Y-axis, Table S4d) and recycling factor (Rec^X, right Y-axis, Table S4e) for macronutrients and the plant beneficial element Si. *The DEF^X (Eq. (11)) quantifies the dissolved riverine loss of X from the ecosystem relative to its net release from the regolith. The Rec^X (Eq. (12)) quantifies how often an element X is bio-utilised by plants after its release by chemical weathering.*

Biogeosciences Discuss., doi:10.5194/bg-2016-521, 2017
Manuscript under review for journal Biogeosciences
Published: 16 January 2017

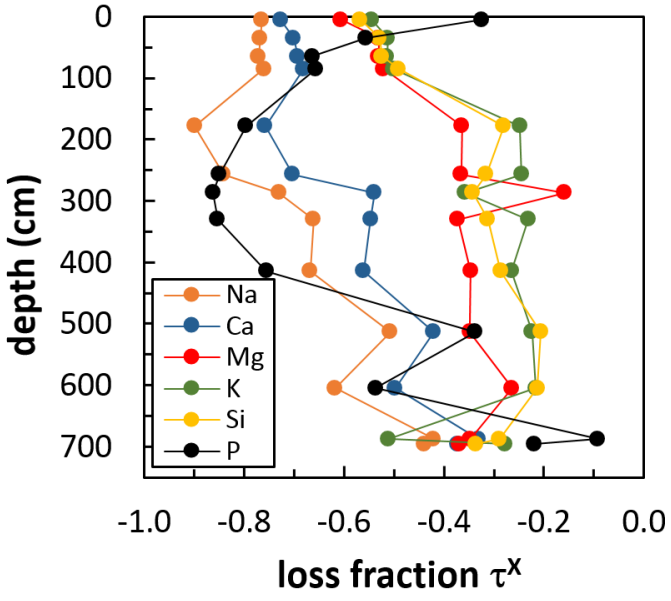

Fig. 6: Loss fraction (τ^x) for macronutrients, the plant essential element Si, and Na of the soil-saprolite depth profile BP. *A τ value < 0 indicates elemental loss in soil/saprolite relative to unweathered bedrock.*

715

Biogeosciences Discuss., doi:10.5194/bg-2016-521, 2017
Manuscript under review for journal Biogeosciences
Published: 16 January 2017

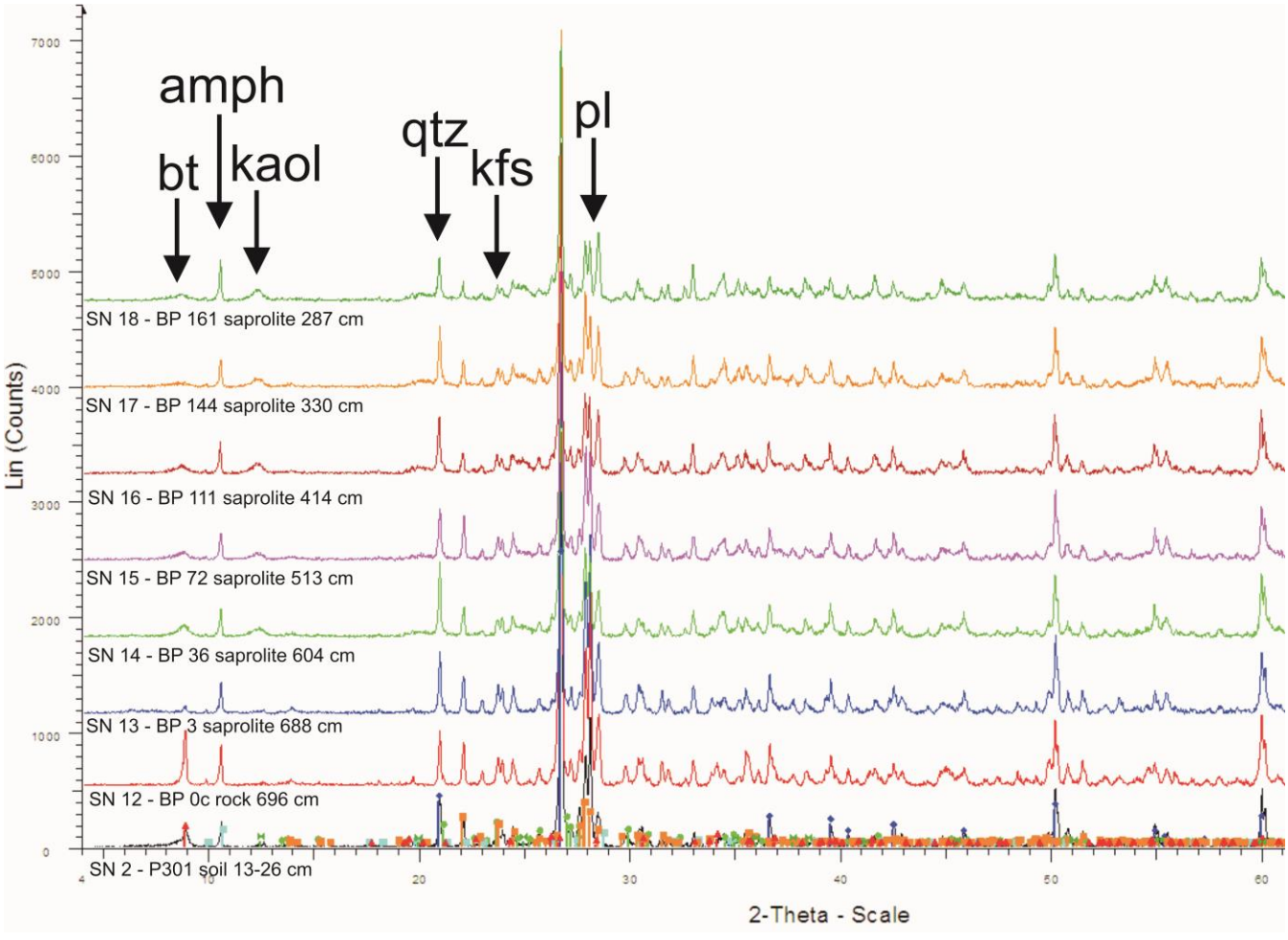

Fig. B1: X-ray diffraction (XRD) pattern of bulk soil, bulk saprolite, and bulk bedrock. *Major reflections of primary (bt = biotite, amph = amphibole, qtz = quartz, kfs = K-feldspar, pl = plagioclase) and secondary minerals (kaol = kaolinite) are indicated.*